A Chemical Mechanistic Path Leads the Way to Cellular Argpyrimidine

Vo Tri Tin Pham, Suprama Datta, Amy C. Sterling, Stefan M. Hansel, Rebecca A. Scheck*

Tufts University, Department of Chemistry, 62 Talbot Ave, Medford MA 02155 USA

KEYWORDS advanced glycation end-product · glycation · methylglyoxal · protein modification · proteomics

ABSTRACT: Argpyrimidine (APY) is a methylglyoxal-derived advanced glycation end-product (AGE) that has been associated with multiple diseases. As APY formation occurs without an enzyme, it remains exceptionally difficult to pinpoint where APY is likely to be found, both on individual proteins and in cells. In this study, we used a peptide model system and mass spectrometry analysis to investigate the chemical mechanism through which APY forms from methylglyoxal (MGO), a biologically relevant glycating agent. Consistent with other proposed APY formation mechanisms, our results show that that another AGE, tetrahydropyrimidine (THP) is a direct precursor to APY. However, our results rule out previously proposed reductone or oxidative decarboxylation mechanisms. Instead, we show that a formal oxidation step is not required, and that formate, not CO_2 is released. We further show the potential for a nearby residue such as Tyr to assist in the APY formation mechanism by acting as a general base. These experiments revealed that phosphorylated Tyr or Ser residues could also promote equivalent levels of APY formation, despite introducing additional negative charges that we previously showed to impede glycation. Guided by these mechanistic insights and newly defined role for phosphorylated residues on glycation substrates, we performed quantitative bottom-up proteomics analysis for MGO-treated cells. Gene ontology analysis for AGE-modified proteins revealed significant enrichment of phosphorylation-related terms (e.g. kinase activity or protein phosphorylation) for APY, while other Arg post-translational modifications did not. Collectively, these data define a chemical mechanistic path to APY and suggest significant crosstalk between cellular phosphorylation and glycation events including APY formation.

Introduction

Argpyrimidine (APY) is one of a group of nearly 40 protein post-translational modifications (PTMs) known as advanced glycation end-products (AGEs).[1–3] AGEs are hallmarks of aging and disease that form non-enzymatically on Lys, the N-terminus, or—in the case of APY—on Arg residues.[1–3] Despite a relatively high pK_a, the Arg guanidino group reacts selectively with α-oxoaldehydes such as the biological glycating agent methylglyoxal (MGO), forming multiple AGEs.[4–6] In addition to APY, these include the methylglyoxal-derived hydroimidazolone isomers (MGH-1, -2, & -3), dihydroxyimidazolidine (MGH-DH), carboxyethylarginine (CEA), and tetrahydropyrimidine (THP) (**Figure 1**). Although there is accumulating evidence that certain AGEs, especially the MGH isomers and CEA, lead to specific biological consequences,[7–12] far less is known about the biology of APY. Several reports have correlated APY with cellular processes like apoptosis, autophagy, or chaperone activity, and a few have shown its association with diseases like brunescent cataractous lens, filial amyloidotic polyneuropathy, or cancer.[13–21] Still, there are virtually no causal connections that link APY to specific biological consequences.

These open questions persist because APY has been notoriously difficult to track due to a lack of highly specific tools, and an unknown formation mechanism. Given that APY requires more than a single MGO molecule to form, it could be particularly relevant under hyperglycemic conditions. Additionally, it has been proposed that APY formation also depends on oxidative stress, suggesting that it could be a critical link between glycation and other cellular stresses.[20,22,23] It is therefore essential to understand APY's formation mechanism to pinpoint the features that influence its formation and the locations—both on proteins and in cells—where APY is more likely to accumulate.

Previous work in our lab has shown that specific Arg-derived AGEs depend not only on MGO concentrations, but also the surrounding chemical microenvironment.[4,5] We have shown that several of these Arg-derived AGEs are mechanistically connected and can interconvert.[4] In this work, we use a

peptide model system to determine chemical features that favor APY formation. We show that although APY is generated more slowly than other AGEs, it is quite a stable AGE once formed. We also confirm that tetrahydropyrimidine (THP) is a direct precursor to APY, and we propose a new APY formation mechanism that involves an initial retro-aldol step, ultimately generating formate as a byproduct, rather than an oxidative decarboxylation. We further demonstrate that the presence of a nearby Tyr can facilitate APY formation. These experiments also revealed that phosphorylated Tyr or Ser residues could also facilitate APY formation, despite adding substantial negative charges that we have previously shown to inhibit glycation. These results prompted us to conduct quantitative proteomics experiments investigating APY formation in live cells treated with MGO, enabling us to draw a previously unknown connection between AGE formation and phosphorylation in a cellular context. These findings provide essential mechanistic insights that are greatly needed for future studies that seek to develop chemical or fluorescent tools that can be used to predict, sense, and study glycation events in living cells.

Results

Although APY requires two molecules of MGO (72.06 Da), its mass change ([M+80]) does not clearly match with an obvious mechanism involving loss or gain of water, as is the case for other AGEs like MGHs, MGH-DH, or CEA.[1] This has made it particularly challenging to define the APY formation mechanism.[3,24,25] Prior work from our lab and others' points to tetrahydropyrimidine (THP) as a possible precursor to APY.[4,24,25] Specifically, we found that by observing AGE distributions for up to 4 weeks of incubation with MGO, there was an inversely proportional relationship between APY and THP over time.[4] We therefore initiated this study by incubating our previous hit peptide (Ac-LESRHYA, peptide **1**, 1 mM) with two equivalents (2 mM) of MGO, expecting that APY levels would increase at higher MGO concentrations. However, little to no APY was observed (< 2% APY), even after 72 hours of treatment, despite total glycation nearing 100% after 48 h, as assessed by liquid chromatography-mass spectrometry (LC-MS) (**Fig. 2A&B**). We also screened two additional peptide sequences that we previously identified

as APY-modified using MGO-treated proteins *in vitro* (**Fig. S1**). Even when increasing MGO concentrations to 3 mM, there was little to no (< 2%) APY after 48 hours across all treated peptides, signifying that APY formation is largely independent of initial MGO concentrations, despite requiring two MGO equivalents to form.

Nonetheless, the major difference in AGE distribution at 3 and 24 h allowed us to test the hypothesis that an [M+144] adduct (likely THP) was a precursor to APY. To do so, we incubated peptide **1** with 2 mM MGO for either 3 h or 24 h. After this initial incubation, we diluted the reaction mixture 100X in the same buffer and compared the resulting AGE distributions at several post-dilution time points (**Fig. 2C—E**). Since dilution markedly slows MGO addition, this protocol diminishes new AGE formation on already glycated peptides, thereby enabling the clear observation of rearrangements between AGEs. At 3 h, MGH-DH (37.1 ± 3.4 %) was the predominant AGE, but at 24 h, THP (51.0 ± 9.4 %) became the predominant AGE. While dilution of the 3 h incubation did not yield any APY even at 48 h post dilution (**Figure 2C&E**), we observed a substantial increase in [M+80] levels when the 24 h incubation was diluted, reaching 10.0 ± 0.3 % APY after 48 h post dilution (**Fig. 2D&E**). These data confirmed the hypothesis that THP is a precursor to APY.

Despite defining THP as an intermediate along the APY formation pathway, persistent low levels of APY remained a consistent technical challenge. Seeking to increase APY levels, we conducted a temperature scan in which we incubated peptide **1** with 2 mM MGO for 24 hours, using temperatures ranging from 37–70 °C (**Fig. 3A**). We found that between 37 °C and 45 °C, there was hardly any change in the AGE distribution. Across the entire range of temperatures used, other AGEs, like MGH-1 and CEA, stayed fairly constant, with only slight increases at higher temperatures. However, at 55 °C, we began to observe a notable increase in APY that was concomitant with reduced THP levels. APY levels peaked at 53.1 ± 12.1 % at 60 °C, becoming the predominant AGE in just 24 hours. Due to high levels of APY

observed at 60 °C, we were able to confirm its identity using its characteristic fluorescence wavelengths (ex = 320 nm, em = 385 nm) (**Fig. S2**).[3,20,25,26]

To further investigate the relationship between APY and THP, we extended the reaction at 60 °C across multiple time points. At 60 °C, the reaction quickly reached 88.1 ± 1.9 % total glycation in only 3 h. From this, we conclude that most of the free MGO is quickly consumed, producing THP as the major early AGE (54.3 ± 1.8 % of total glycation) (**Fig. 3C**). APY levels began to increase after 2 h of incubation, with a precipitous increase (from 0.0 % to 24.5 ± 5.5 %) between 3 and 6 h. During this same time frame, a concomitant, proportional decrease in [M+144] levels was observed, providing unambiguous assignment of THP as a precursor to APY.

Additionally, comparison of the AGE distributions at 37 °C and 60 °C revealed APY is a stable AGE. After heating at 60 °C for 24 h, only MGH-1 and APY remained in appreciable quantities, while other AGEs, like CEA and THP, disappeared, presumably due to rearrangements to other AGEs (**Fig. 3D**). We have also shown that while elevated temperatures increase APY levels at earlier time points, APY formation is still dependent on the sequence identity (**Fig. S3**). Thanks to high levels of APY observed, we also conducted stability studies for purified APY on peptide **1** (peptide $\mathbf{1}^{\mathbf{APY}}$) and showed that APY on a short peptide is fairly stable under physiological conditions (**Fig. S4**). Importantly, these findings not only identify conditions at which APY can become a major AGE, but they also suggest that the rearrangement of THP into APY likely involves a high energy activation barrier that can be overcome by the addition of heat.

Next, we sought to understand possible mechanisms through which this rearrangement could take place. The most cited APY formation mechanism involves the generation of a reductone from two MGO, which then reacts with Arg to form APY (**Fig. S5**).[3] In this model, preincubation of MGO alone would be expected to generate the reductone, consequently leading to faster APY formation once added to peptide. We found that preincubation, even at strongly acidic pH and elevated temperatures (60 °C), did not

promote any further APY formation upon addition to peptide **1** (**Fig. S6 & S7**). These results are therefore inconsistent with reductone formation as a plausible model for APY formation in physiological conditions. Another proposed mechanism suggests that MGH-3 rearranges to form APY, presumably through a THP intermediate.[24] However, our substantial data using peptide **1** shows that the only MGH isomer consistently identified is MGH-1, suggesting that MGH-3 is not a prerequisite for APY formation.[4] Because MGH-3 is known to be less stable than MGH-1, it is most likely that this observation aligns with other proposals (including ours) that THP rearranges to form APY.

Previous proposals have hypothesized that THP rearranges to APY through a pathway involving oxidation, followed by decarboxylation and then dehydration (**Fig. S5**).[24,25] To evaluate the feasibility of an oxidative decarboxylation from THP, we first sought to understand whether APY could form under O_2-free conditions. We scrupulously degassed all reaction components and used a glovebox to assemble and seal glycation reactions inside an N_2 sparged (O_2 < 4 ppm) scintillation vial that was further sealed prior to incubation. The resulting APY levels observed were identical in the presence or absence of oxygen (**Fig. S8**), suggesting that a formal oxidation step may not be required. However, our studies were performed using commercial sources of MGO, which may contain impurities. To see if any potential impurities were contributing to APY formation, we synthesized MGO using an established Riley oxidation protocol (**Fig. S9**).[27] We found that there was no difference in APY formation between a freshly synthesized stock of MGO and commercial MGO. We also evaluated the role of buffer and salt concentrations, and found negligible differences (**Fig. S10**).

As we could not attribute the source of oxidation required in the previously proposed mechanism, we considered other potential mechanisms in which THP could rearrange to form APY. We identified a possible alternative pathway (**Figure 4**) in which initial deprotonation of the hydroxyl group at C5 promotes a retro-aldol ring opening. Next, hydration of the aldehyde followed by deprotonation generates a geminal enediol at C5, followed by subsequent ring closure and another dehydration and retro-aldol step

to generate the pyrimidine ring. This proposed mechanism generates formic acid as a byproduct of THP rearrangement. Supporting this proposal, we used an enzyme coupled assay to detect formic acid in reactions of peptide **1** with 2 mM MGO after 24 h (F**ig. S11**). Our results indicate that formic acid is a byproduct of our proposed mechanism, though we also found that it is not necessarily exclusive to APY formation.

In further support of this idea, our proposed mechanism has an intermediate that is a tautomer of CEA, allowing us to hypothesize that besides THP and MGH-3, CEA could be another precursor to APY. To evaluate this idea, we purified CEA and MGH-1 modified peptide **1** (peptides $\mathbf{1}^{\mathbf{CEA}}$ and $\mathbf{1}^{\mathbf{MGH\text{-}1}}$, respectively). At pH 7.3, without any additional MGO added, we observed only modest conversion from $\mathbf{1}^{\mathbf{MGH\text{-}1}}$ to $\mathbf{1}^{\mathbf{CEA}}$ with little degradation to peptide **1**, consistent with our previous results.[4] However, upon treatment with additional equivalents of MGO, we found that only peptide $\mathbf{1}^{\mathbf{CEA}}$ produced APY (**Fig. S12**).

To further evaluate the feasibility of our proposed mechanism, we predicted that a general base would be necessary for the initial deprotonation step that promotes ring opening, as well as for subsequent ring closure and dehydration (**Figure 4**). Using a pH scan, we found that APY levels increased between pH 7.3–11 (**Figure 5A&B**). There was a particularly large jump in APY levels between pH 10 (3.3 ± 1.4 %) and pH 11 (20.3 ± 1.1 %), prompting us to conduct a narrower pH scan at 0.2 increments between pH 10 and 11. In this range, we found that APY levels increased steadily, peaking at pH 11 (20.3 ± 1.1 % of total glycation) (**Fig. 5C**). There was a sharp transition between pH 10.2 and 10.4, suggesting a strong correlation with the protonation state of the nearby Tyr residue (pK_a 10.3).[28–30] These results suggest that, for peptide **1**, Tyr plays an active role in the APY formation mechanism.

To test the hypothesis that Tyr phenoxide facilitates APY formation, we synthesized variants of peptide **1** that incorporated noncanonical Tyr derivatives with lowered phenolic pK_a's. Specifically, 3-fluorotyrosine (peptide $\mathbf{1}^{\mathbf{F}}$) and 3,5-difluorotyrosine (peptide $\mathbf{1}^{\mathbf{FF}}$) were chosen because of their pK_a values (8.4 and 7.2, respectively) (**Fig. 4D**).[31] These peptides were reacted with 2 mM MGO across a range of

pH between 7.3 and 12 (**Fig. 4D** and **Fig. S13**), revealing maximal APY levels at pH 11 for all three peptides. However, when normalized to account for differences in total glycation levels, we found that proportional APY levels at pH 7.3 were greatest for peptide $\mathbf{1^{FF}}$ (5.0 ± 0.3%), followed by $\mathbf{1^{F}}$ (1.3 ± 1.5%), and then peptide **1** (0.6 ± 0.4%) (**Fig. S13**). These results demonstrate the importance of the nearby Tyr as a facilitator for THP rearrangement into APY, matching our hypothesis that Tyr can act as a general base that facilitates APY formation.

Following the same logic, we next considered if phosphorylated Tyr—or perhaps even Ser or Thr—might also act as a general base promoting APY formation. Phosphorylated Tyr has experimental pK_{a2} values ranging between 4.0 to 6.1.[32] Thus, we synthesized peptide $\mathbf{1^{pY}}$ that contains pTyr in place of Tyr. After glycation with 2 mM MGO at pH 7.3 at 60 °C for 24 h, there were hardly any differences in total glycation and APY levels between peptide **1** (52.8 ± 4.5 % [M+80] at 24 h) and $\mathbf{1^{pY}}$ (48.8 ± 0.6 % [M+80] at 24 h) (**Fig. 5E & Fig. S14**). We performed a similar set of experiments using a peptide **1** variant with phosphorylated Ser (peptide $\mathbf{1^{pS}}$), and found that these also produced comparable levels of glycation (50.9 ± 0.3%) after 24 h, despite the addition of up to two negative charges (**Fig. 5E & Fig. S14**). Accordingly, these results imply that nearby phosphorylation may be helpful for glycation, and based on our proposed mechanism, could be particularly important for APY formation in a cellular context.

Guided by these mechanistic insights, we performed a quantitative proteomics experiment on HEK-293T cells treated with or without MGO. Our mechanistic studies have shown that APY can accumulate at longer times or using higher MGO concentrations. Therefore, we opted to treat cells with 2 mM MGO for 24 h to ensure that we could induce APY formation. Several reagents, such as dithiothreitol (DTT) and iodoacetamide, used in proteomic experiments were tested for their effects on AGE distribution and APY formation and found to have no interference (**Fig. S15**). Additionally, as there are no highly specific antibodies available to enrich APY (**Fig. S16**), we chose to label an unenriched cell lysate with isobaric tandem mass tags, allowing us to evaluate the distribution of multiple AGEs using

quantitative bottom-up proteomics, including the MGH isomers ([M+54]), APY ([M+80]), THP ([M+144]), and an [M+72] adduct that could correspond to MGH-DH, CEA, or CEL. Using this approach, we identified 7210 total proteins and 56490 peptides across all conditions tested, and found 478 unique peptides that were AGE-modified upon treatment with 2 mM MGO. This dataset shows significant similarity to other MGO-treated proteomic datasets, with AGE modifications enriched on proteins involved in processes such as protein folding and spliceosome function, along with several modified histone and heat shock proteins.[9,10,33,34]

Upon meticulous inspection of our dataset, we manually removed any glycated peptides that were assigned with a modified Arg at the end of the sequences, as we and others have previously shown that glycated Arg cannot be cleaved by trypsin. After data processing, this decreased the total list of AGE-modified peptides to 204 plausible AGE-modified hits. Without any enrichment that could bias the AGE distribution, we found that APY was the predominant AGE in the MGO-treated condition (57 unique peptides, 28%), followed by THP (53 unique peptides, 26%), and then the MGH isomers and CEA/MGH-DH (47 unique peptides, 23% for each) (**Fig. 6B**). Although our dynamic modification for [M+72] (mass change 72.021) was set for both Arg and Lys, with the expectation that CEL might also be present, we only observed modification on Arg, corresponding to MGH-DH and/or CEA. Though glycation is largely driven by chemical microenvironments that include 3D protein structure and is therefore unlikely to have a strong consensus sequence, we were able to obtain consensus features for each AGE and were heartened to observe Thr, Ser, and Tyr in the consensus features of APY, suggesting potential crosstalk between nearby phosphorylation sites and the propensity of Arg to become glycated (**Fig. S17**).

Next, we performed gene ontology (GO) analysis for the APY-modified set of proteins. In both the molecular function (MF) and biological process (BP) annotations, APY-containing proteins showed a statistically significant enrichment of terms related to phosphorylation, including protein phosphorylation (BP) and multiple kinase activities (MF), despite having a relatively low number of protein IDs (**Fig. 6C**).

We found that none of the other AGE sets showed an enrichment of protein phosphorylation (BP) or kinase activity (MF) (**Fig. S18—S21**), and the APY-modified set was the only set to exhibit protein serine/threonine kinase activity, implying a connection between APY formation and phosphorylation in a cellular context.

Building on this observation, we further investigated the set of 57 modified APY-containing peptides, which were observed across the entire range of AGEs when ranked by abundance (**Fig. 6D**). We focused in particular on the eight highest confidence APY-modified peptides that exhibited statistically significant increases in abundance upon MGO treatment across all three biological replicates (**Fig. 6D&E** and **Fig. S22—S26**). Data imputation and statistical analysis were performed according to published protocols.[35] Among these peptides, one was also identified with a phosphorylated residue nearby the APY-modified site, corresponding to HOXA6 (hit 3) (R156, R157 with nearby pS153).

Of the remaining seven high confidence APY hits, six were previously reported to be phosphorylated, and some are known to be regulated by phosphorylation.[36] For example, phosphorylation of MAP4 (hit 2) has been reported to affect microtubule properties and cell cycle progression, while TIAL1 (hit 5) has also been found to be phosphorylated following DNA damage, and phosphorylation of PKD1 (hit 6) triggers its membrane dissociation and subsequent entry into the nucleus.[37–39] Additionally, phosphorylation of UHRF1 maintains protein stability, subcellular localization, and epigenetic regulation (hit 1).[40] Careful inspection of our data revealed that UHRF1 was APY-modified at R207, which is close to T210, a known phosphorylated site previously reported to be essential in maintaining UHRF1 stability, though phosphorylated T210 was not observed in our dataset.[41]

Similarly, S358, close in sequence to APY-modified R353, on ELAVL3 (hit 7) has also been shown to be phosphorylated.[36] We also found two APY modifications on the C-terminal domain of PKD-1 (R4107, R4109), which contains 4 Tyr residues (Y4110, Y4118, Y4127, Y4237) and 2 putative Ser sites (S4169, S4252) that are susceptible to phosphorylation. Multiple *in vitro* studies have revealed Y4237 and

S4252 to be targets of phosphorylation by pp60c-src and PKA, respectively, and shown endogenous PKD-1 to be phosphorylated at tyrosine.[42–44] Together, our data show several APY modifications on Arg residues close to known phosphorylation sites, consistent with the potential for crosstalk between cellular APY and phosphorylation events.

However, as APY (mass change 80.026) is quite close in mass to phosphorylation (mass change 79.966), we also queried our dataset for phosphorylation and found that the list of proteins generated had some overlap with the set of APY-modified targets, but the overall list of IDs was quite different, confirming that the relatively similar mass changes did not produce artifactual hits. We also found that the phosphorylated set (220 proteins) showed substantial overlap (30 proteins) with the AGE-modified set of proteins (180 proteins). To evaluate the possibility that crosstalk between nearby phosphorylation could promote AGE formation (especially for APY and MGHs), we performed a parallel analysis for other common Arg PTMs, including dimethylation and acetylation (**Fig. 6F** and **Fig. S27&S28**). We found 99 unique peptides with dimethylated Arg and 30 unique peptides with acetylated Arg. Importantly, the phosphorylated set of proteins did not substantially overlap with those that were observed to be dimethylated (9 IDs) or acetylated (2 IDs) (**Fig. 6F**).

Overall, our proteomic dataset supported our *in vitro* experiments, suggesting that APY formation is promoted by phosphorylated residues that act as general bases to facilitate THP rearrangement into APY **(Fig. 4)**. However, in our prior work we also found a nearby general base to facilitate MGH-1 formation on peptide **1,** although we did not explore phosphate-modified side chains.[4] We therefore evaluated the glycation of peptides **1**, $\mathbf{1^{pY}}$, $\mathbf{1^{pS}}$, and $\mathbf{1^{pSpY}}$ at 37 °C and over extended time periods. Supporting our findings at 60 °C, these studies showed that APY levels to be fairly similar across all times for peptides **1**, $\mathbf{1^{pY}}$, and $\mathbf{1^{pS}}$. However, MGH-1 levels were noticeable increased—especially at earlier times—for the phosphorylated substrates. Additionally, introduction of up to two negative charges on peptide $\mathbf{1^{pY}}$ and $\mathbf{1^{pS}}$ did not affect overall glycation but led to increased APY and MGH-1 formation.

However, at both lower and elevated temperatures, the introduction of four negative charges on peptide **1**$^{\mathbf{pSpY}}$ decreased overall glycation, and showed a substantial preference for MGH-1 over APY formation (**Fig. S29**). Taken together, these data support a model in which crosstalk with protein phosphorylation could have an important, but previously underappreciated role in regulating cellular glycation events.

Discussion

Herein we have used a peptide model system to determine a chemical mechanism for APY formation. Although appreciated for its unique fluorescence properties,[3,24,45] APY has been difficult to study as it was not previously known how to produce it in experimentally convenient quantities from the reaction of Arg and MGO.[17,18,20] Our results indicate that APY formation depends surprisingly little on initial MGO concentrations, and instead greatly depends on other factors, including sequence identity, reaction pH, and temperature, each of which can help to overcome a relatively high energy rate determining step. Through these studies, we discover that APY is quite stable and identify conditions under which APY becomes the predominant AGE, which to our knowledge, has not been previously reported. These findings alone provide an important technical advance that will greatly facilitate future studies on APY.

Additionally, our proposed mechanism relies on fundamental concepts of organic chemistry and provides concrete experimental evidence that reconciles several previous, conflicting mechanisms proposed for APY. While others have suggested that THP is a precursor to APY, our newly proposed mechanism circumvents the need for an unexplained, mysterious oxidation step by recognizing that THP possesses a β-hydroxycarbonyl, a common feature in retro-aldol substrates. Indeed, the retro-aldol reaction is one of the most important organic reactions in sugar fragmentations, including those in physiological systems.[46–48] Several known retro-aldol enzymes use Tyr as a general base,[49–51] which aligns with our results showing noncanonical Tyr variants with decreased phenolic pK_a to promote APY formation. Our mechanism also connects APY formation to the emancipation of formate, a major reactive

species in one-carbon metabolism that is involved in numerous biological processes.[52–54] While there has been some prior work connecting the metabolic processing of MGO to formate generation,[55–59] our results suggest that cellular glycation events themselves, including but not limited to APY formation, may also contribute to the cellular formate pool.

Encouragingly, our dataset shows that APY is likely to be a major AGE in cells. We suspect the prevalence of APY has seemingly been underestimated in previous studies due to the use of enrichment protocols that are poorly suited to capture APY. Our mechanistic studies therefore not only provide much needed insights into APY formation under physiologically relevant conditions, but also reveal critical aspects of the glycation landscape. In future studies, we plan to leverage this information to generate novel chemical tools that can be used to track and/or control APY formation in living cells, including the development of tools that harness APY's unique autofluorescent properties for bioconjugation and to assist in the study of APY biology.

This study also reveals the potential for significant crosstalk between glycation and phosphorylation, showing the presence of nearby phosphorylated side chains to enhance, and potentially bias, particular AGEs to form. Our experiments examine the ability of phosphorylated residues (pSer & pTyr) to promote formation of certain AGEs, particularly that of MGH-1 and APY, despite introducing additional negative charges previously shown to hamper glycation.[4,5] These peptide data are also supplemented with quantitative proteomics analysis on MGO-treated cells, revealing a similar connection between phosphorylation and glycation, that was notably missing with other Arg PTMs like acetylation and dimethylation. While inorganic phosphate has long been known to enhance glycation,[60] and MGO has been shown to stimulate phosphorylation,[61–64] we have not been able to find any reports suggesting that nearby phosphorylated sites increase glycation. Therefore, our study is the first to show that glycation may be coincident with phosphorylation on the same substrates, and that the presence of these nearby

phosphates may bias the resulting AGE distribution. Our future work will seek to fully elucidate both the chemical and biological significance of this phenomenon.

ASSOCIATED CONTENT

Supporting Information

All AGE peptides from proteomic analysis of treated cells in Excel file

AUTHOR INFORMATION

Corresponding Author

* rebecca.scheck@tufts.edu

Funding Sources

This work was supported by National Institutes of Health grant R01GM132422 to R.A.S, as well as by a gift to the Scheck Lab from J. Kanagy, and a gift to the Scheck Lab from J. Fickel.

ACKNOWLEDGMENT

We would like to express our gratitude to Dr. Krishna Kumar and Dr. Luke Davis for project guidance and to the Zhang Lab (Tufts University Department of Chemistry) for assistance with experiments conducted inside the glovebox.

ABBREVIATIONS

AGE, advanced glycation end-product; APY, argpyrimidine; MGO, methylglyoxal; MGH-1, -2, & -3, hydroimidazolone isomers; MGH-DH, dihydroxyimidazolidine; CEA, carboxyethylarginine; THP, tetrahydropyrimidine; LC-MS, liquid chromatography-mass spectrometry; HPLC, high-performance liquid chromatography; TMT, tandem mass tag; GO analysis, gene ontology analysis.

REFERENCES

(1) Martin, M. S.; Jacob-Dolan, J. W.; Pham, V. T. T.; Sjoblom, N. M.; Scheck, R. A. The Chemical Language of Protein Glycation. *Nat Chem Biol* **2025**, *21* (3), 324–336. https://doi.org/10.1038/s41589-024-01644-y.

(2) Monnier, V. M.; Cerami, A. Nonenzymatic Browning in Vivo: Possible Process for Aging of Long-Lived Proteins. *Science* **1981**, *211* (4481), 491–493. https://doi.org/10.1126/science.6779377.

(3) Shipanova, I. N.; Glomb, M. A.; Nagaraj, R. H. Protein Modification by Methylglyoxal: Chemical Nature and Synthetic Mechanism of a Major Fluorescent Adduct. *Archives of Biochemistry and Biophysics* **1997**, *344* (1), 29–36. https://doi.org/10.1006/abbi.1997.0195.

(4) McEwen, J. M.; Fraser, S.; Guir, A. L. S.; Dave, J.; Scheck, R. A. Synergistic Sequence Contributions Bias Glycation Outcomes. *Nat Commun* **2021**, *12* (1), 3316. https://doi.org/10.1038/s41467-021-23625-8.

(5) Sjoblom, N. M.; Kelsey, M. M. G.; Scheck, R. A. A Systematic Study of Selective Protein Glycation. *Angew Chem Int Ed* **2018**, *57* (49), 16077–16082. https://doi.org/10.1002/anie.201810037.

(6) Ahmed, N.; Dobler, D.; Dean, M.; Thornalley, P. J. Peptide Mapping Identifies Hotspot Site of Modification in Human Serum Albumin by Methylglyoxal Involved in Ligand Binding and Esterase Activity. *Journal of Biological Chemistry* **2005**, *280* (7), 5724–5732. https://doi.org/10.1074/jbc.M410973200.

(7) Trujillo, M. N.; Galligan, J. J. Reconsidering the Role of Protein Glycation in Disease. *Nat Chem Biol* **2023**, *19* (8), 922–927. https://doi.org/10.1038/s41589-023-01382-7.

(8) Zheng, Q.; Omans, N. D.; Leicher, R.; Osunsade, A.; Agustinus, A. S.; Finkin-Groner, E.; D'Ambrosio, H.; Liu, B.; Chandarlapaty, S.; Liu, S.; David, Y. Reversible Histone Glycation Is Associated

with Disease-Related Changes in Chromatin Architecture. *Nat Commun* **2019**, *10* (1), 1289. https://doi.org/10.1038/s41467-019-09192-z.

(9) Galligan, J. J.; Wepy, J. A.; Streeter, M. D.; Kingsley, P. J.; Mitchener, M. M.; Wauchope, O. R.; Beavers, W. N.; Rose, K. L.; Wang, T.; Spiegel, D. A.; Marnett, L. J. Methylglyoxal-Derived Posttranslational Arginine Modifications Are Abundant Histone Marks. *Proc. Natl. Acad. Sci. U.S.A.* **2018**, *115* (37), 9228–9233. https://doi.org/10.1073/pnas.1802901115.

(10) Alhujaily, M.; Abbas, H.; Xue, M.; De La Fuente, A.; Rabbani, N.; Thornalley, P. J. Studies of Glyoxalase 1-Linked Multidrug Resistance Reveal Glycolysis-Derived Reactive Metabolite, Methylglyoxal, Is a Common Contributor in Cancer Chemotherapy Targeting the Spliceosome. *Front. Oncol.* **2021**, *11*, 748698. https://doi.org/10.3389/fonc.2021.748698.

(11) Bollong, M. J.; Lee, G.; Coukos, J. S.; Yun, H.; Zambaldo, C.; Chang, J. W.; Chin, E. N.; Ahmad, I.; Chatterjee, A. K.; Lairson, L. L.; Schultz, P. G.; Moellering, R. E. A Metabolite-Derived Protein Modification Integrates Glycolysis with KEAP1–NRF2 Signalling. *Nature* **2018**, *562* (7728), 600–604. https://doi.org/10.1038/s41586-018-0622-0.

(12) Bierhaus, A.; Fleming, T.; Stoyanov, S.; Leffler, A.; Babes, A.; Neacsu, C.; Sauer, S. K.; Eberhardt, M.; Schnölzer, M.; Lasitschka, F.; Neuhuber, W. L.; Kichko, T. I.; Konrade, I.; Elvert, R.; Mier, W.; Pirags, V.; Lukic, I. K.; Morcos, M.; Dehmer, T.; Rabbani, N.; Thornalley, P. J.; Edelstein, D.; Nau, C.; Forbes, J.; Humpert, P. M.; Schwaninger, M.; Ziegler, D.; Stern, D. M.; Cooper, M. E.; Haberkorn, U.; Brownlee, M.; Reeh, P. W.; Nawroth, P. P. Methylglyoxal Modification of Nav1.8 Facilitates Nociceptive Neuron Firing and Causes Hyperalgesia in Diabetic Neuropathy. *Nat Med* **2012**, *18* (6), 926–933. https://doi.org/10.1038/nm.2750.

(13) Antognelli, C.; Mezzasoma, L.; Fettucciari, K.; Talesa, V. N. A Novel Mechanism of Methylglyoxal Cytotoxicity in Prostate Cancer Cells. *The International Journal of Biochemistry & Cell Biology* **2013**, *45* (4), 836–844. https://doi.org/10.1016/j.biocel.2013.01.003.

(14) Antognelli, C.; Gambelunghe, A.; Muzi, G.; Talesa, V. N. Peroxynitrite-Mediated Glyoxalase I Epigenetic Inhibition Drives Apoptosis in Airway Epithelial Cells Exposed to Crystalline Silica via a Novel Mechanism Involving Argpyrimidine-Modified Hsp70, JNK, and NF-κB. *Free Radical Biology and Medicine* **2015**, *84*, 128–141. https://doi.org/10.1016/j.freeradbiomed.2015.03.026.

(15) Kim, J.; Kim, O. S.; Kim, C.-S.; Sohn, E.; Jo, K.; Kim, J. S. Accumulation of Argpyrimidine, a Methylglyoxal-Derived Advanced Glycation End Product, Increases Apoptosis of Lens Epithelial Cells Both *in Vitro* and *in Vivo*. *Exp Mol Med* **2012**, *44* (2), 167. https://doi.org/10.3858/emm.2012.44.2.012.

(16) Li, S.; Yang, D.; Gao, X.; Yao, S.; Wang, S.; Zhu, J.; Shu, J. Argpyrimidine Bonded to RAGE Regulates Autophagy and Cell Cycle to Cause Periodontal Destruction. *Journal Cellular Physiology* **2022**, *237* (12), 4460–4476. https://doi.org/10.1002/jcp.30886.

(17) Matveenko, M.; Cichero, E.; Fossa, P.; Becker, C. F. W. Impaired Chaperone Activity of Human Heat Shock Protein Hsp27 Site-Specifically Modified with Argpyrimidine. *Angew Chem Int Ed* **2016**, *55* (38), 11397–11402. https://doi.org/10.1002/anie.201605366.

(18) Mukherjee, S.; Vogl, D. P.; Becker, C. F. W. Site-Specific Glycation of Human Heat Shock Protein (Hsp27) Enhances Its Chaperone Activity. *ACS Chem. Biol.* **2023**, *18* (8), 1760–1771. https://doi.org/10.1021/acschembio.3c00214.

(19) Padayatti, P. S.; Ng, A. S.; Uchida, K.; Glomb, M. A.; Nagaraj, R. H. Argpyrimidine, a Blue Fluorophore in Human Lens Proteins: High Levels in Brunescent Cataractous Lenses. *Invest Ophthalmol Vis Sci* **2001**, *42* (6), 1299–1304.

(20) Gomes, R.; Sousa Silva, M.; Quintas, A.; Cordeiro, C.; Freire, A.; Pereira, P.; Martins, A.; Monteiro, E.; Barroso, E.; Ponces Freire, A. Argpyrimidine, a Methylglyoxal-Derived Advanced Glycation End-Product in Familial Amyloidotic Polyneuropathy. *Biochemical Journal* **2005**, *385* (2), 339–345. https://doi.org/10.1042/BJ20040833.

(21) Van Heijst, J. W. J.; Niessen, H. W. M.; Hoekman, K.; Schalkwijk, C. G. Advanced Glycation End Products in Human Cancer Tissues: Detection of N^{ε}-(Carboxymethyl)Lysine and Argpyrimidine. *Annals of the New York Academy of Sciences* **2005**, *1043* (1), 725–733. https://doi.org/10.1196/annals.1333.084.

(22) Kim, J.; Kim, N. H.; Sohn, E.; Kim, C.-S.; Kim, J. S. Methylglyoxal Induces Cellular Damage by Increasing Argpyrimidine Accumulation and Oxidative DNA Damage in Human Lens Epithelial Cells. *Biochemical and Biophysical Research Communications* **2010**, *391* (1), 346–351. https://doi.org/10.1016/j.bbrc.2009.11.061.

(23) Antognelli, C.; Mezzasoma, L.; Mearini, E.; Talesa, V. N. Glyoxalase 1−419C>A Variant Is Associated with Oxidative Stress: Implications in Prostate Cancer Progression. *PLoS ONE* **2013**, *8* (9), e74014. https://doi.org/10.1371/journal.pone.0074014.

(24) Klöpfer, A.; Spanneberg, R.; Glomb, M. A. Formation of Arginine Modifications in a Model System of N^{α} - *Tert* -Butoxycarbonyl (Boc)-Arginine with Methylglyoxal. *J. Agric. Food Chem.* **2011**, *59* (1), 394–401. https://doi.org/10.1021/jf103116c.

(25) Ahmed, N.; Argirov, O. K.; Minhas, H. S.; Cordeiro, C. A. A.; Thornalley, P. J. Assay of Advanced Glycation Endproducts (AGEs): Surveying AGEs by Chromatographic Assay with Derivatization by 6-Aminoquinolyl-N-Hydroxysuccinimidyl-Carbamate and Application to N∈-Carboxymethyl-Lysine- and N∈-(1-Carboxyethyl)Lysine-Modified Albumin. *Biochemical Journal* **2002**, *364* (1), 1–14. https://doi.org/10.1042/bj3640001.

(26) Wilker, S. C.; Chellan, P.; Arnold, B. M.; Nagaraj, R. H. Chromatographic Quantification of Argpyrimidine, a Methylglyoxal-Derived Product in Tissue Proteins: Comparison with Pentosidine. *Analytical Biochemistry* **2001**, *290* (2), 353–358. https://doi.org/10.1006/abio.2001.4992.

(27) Riley, H. L.; Morley, J. F.; Friend, N. A. C. 255. Selenium Dioxide, a New Oxidising Agent. Part I. Its Reaction with Aldehydes and Ketones. *J. Chem. Soc.* **1932**, 1875. https://doi.org/10.1039/jr9320001875.

(28) Oktaviani, N. A.; Pool, T. J.; Kamikubo, H.; Slager, J.; Scheek, R. M.; Kataoka, M.; Mulder, F. A. A. Comprehensive Determination of Protein Tyrosine pKa Values for Photoactive Yellow Protein Using Indirect 13C NMR Spectroscopy. *Biophysical Journal* **2012**, *102* (3), 579–586. https://doi.org/10.1016/j.bpj.2011.12.024.

(29) Harris, T. K.; Turner, G. J. Structural Basis of Perturbed pKa Values of Catalytic Groups in Enzyme Active Sites. *IUBMB Life* **2002**, *53* (2), 85–98. https://doi.org/10.1080/15216540211468.

(30) Aktaş, A. H.; Sanli, N.; Pekcan, G. Spectrometric Determination of pKa Values for Some Phenolic Compounds in Acetonitrile-Water Mixtures. *Acta Chimica Slovenica* **2006**, *53*, 214–218.

(31) Seyedsayamdost, M. R.; Reece, S. Y.; Nocera, D. G.; Stubbe, J. Mono-, Di-, Tri-, and Tetra-Substituted Fluorotyrosines: New Probes for Enzymes That Use Tyrosyl Radicals in Catalysis. *J. Am. Chem. Soc.* **2006**, *128* (5), 1569–1579. https://doi.org/10.1021/ja055926r.

(32) Wojciechowski, M.; Grycuk, T.; Antosiewicz, J. M.; Lesyng, B. Prediction of Secondary Ionization of the Phosphate Group in Phosphotyrosine Peptides. *Biophysical Journal* **2003**, *84* (2), 750–756. https://doi.org/10.1016/S0006-3495(03)74894-2.

(33) Zheng, L.; Boeren, S.; Liu, C.; Bakker, W.; Wang, H.; Rietjens, I. M. C. M.; Saccenti, E. Proteomics-Based Identification of Biomarkers Reflecting Endogenous and Exogenous Exposure to the Advanced Glycation End Product Precursor Methylglyoxal in SH-SY5Y Human Neuroblastoma Cells. *International Journal of Biological Macromolecules* **2024**, *272*, 132859. https://doi.org/10.1016/j.ijbiomac.2024.132859.

(34) Donnellan, L.; Young, C.; Simpson, B. S.; Acland, M.; Dhillon, V. S.; Costabile, M.; Fenech, M.; Hoffmann, P.; Deo, P. Proteomic Analysis of Methylglyoxal Modifications Reveals Susceptibility of Glycolytic Enzymes to Dicarbonyl Stress. *IJMS* **2022**, *23* (7), 3689. https://doi.org/10.3390/ijms23073689.

(35) Aguilan, J. T.; Kulej, K.; Sidoli, S. Guide for Protein Fold Change and *p* -Value Calculation for Non-Experts in Proteomics. *Mol. Omics* **2020**, *16* (6), 573–582. https://doi.org/10.1039/D0MO00087F.

(36) PhosphoSitePlus®. http://www.phosphosite.org/.

(37) Chang, W.; Gruber, D.; Chari, S.; Kitazawa, H.; Hamazumi, Y.; Hisanaga, S.; Bulinski, J. C. Phosphorylation of MAP4 Affects Microtubule Properties and Cell Cycle Progression. *Journal of Cell Science* **2001**, *114* (15), 2879–2887. https://doi.org/10.1242/jcs.114.15.2879.

(38) Chang, J.-K.; Ni, Y.; Han, L.; Sinnett-Smith, J.; Jacamo, R.; Rey, O.; Young, S. H.; Rozengurt, E. Protein Kinase D1 (PKD1) Phosphorylation on Ser203 by Type I P21-Activated Kinase (PAK) Regulates PKD1 Localization. *Journal of Biological Chemistry* **2017**, *292* (23), 9523–9539. https://doi.org/10.1074/jbc.M116.771394.

(39) Osma-Garcia, I. C.; Mouysset, M.; Capitan-Sobrino, D.; Aubert, Y.; Turner, M.; Diaz-Muñoz, M. D. The RNA Binding Proteins TIA1 and TIAL1 Promote Mcl1 mRNA Translation to Protect Germinal Center Responses from Apoptosis. *Cell Mol Immunol* **2023**, *20* (9), 1063–1076. https://doi.org/10.1038/s41423-023-01063-4.

(40) Gu, L.; Fu, Y.; Li, X. Roles of Post-Translational Modifications of UHRF1 in Cancer. *Epigenetics & Chromatin* **2024**, *17* (1), 15. https://doi.org/10.1186/s13072-024-00540-y.

(41) Fu, Y.; Cao, T.; Zou, X.; Ye, Y.; Liu, Y.; Peng, Y.; Deng, T.; Yin, L.; Li, X. AKT1 Regulates UHRF1 Protein Stability and Promotes the Resistance to Abiraterone in Prostate Cancer. *Oncogenesis* **2023**, *12* (1), 1. https://doi.org/10.1038/s41389-022-00446-y.

(42) Geng, L.; Burrow, C. R.; Li, H.-P.; Wilson, P. D. Modification of the Composition of Polycystin-1 Multiprotein Complexes by Calcium and Tyrosine Phosphorylation. *Biochimica et Biophysica Acta (BBA) - Molecular Basis of Disease* **2000**, *1535* (1), 21–35. https://doi.org/10.1016/S0925-4439(00)00079-X.

(43) Li, H.-P.; Geng, L.; Burrow, C. R.; Wilson, P. D. Identification of Phosphorylation Sites in the PKD1-Encoded Protein C-Terminal Domain. *Biochemical and Biophysical Research Communications* **1999**, *259* (2), 356–363. https://doi.org/10.1006/bbrc.1999.0780.

(44) Streets, A.; Ong, A. Post-Translational Modifications of the Polycystin Proteins. *Cellular Signalling* **2020**, *72*, 109644. https://doi.org/10.1016/j.cellsig.2020.109644.

(45) Renard, B.-L.; Boucherle, B.; Maurin, B.; Molina, M.-C.; Norez, C.; Becq, F.; Décout, J.-L. An Expeditious Access to 5-Pyrimidinol Derivatives from Cyclic Methylglyoxal Diadducts, Formation of Argpyrimidines under Physiological Conditions and Discovery of New CFTR Inhibitors. *European Journal of Medicinal Chemistry* **2011**, *46* (5), 1935–1941. https://doi.org/10.1016/j.ejmech.2011.02.037.

(46) Voigt, M.; Smuda, M.; Pfahler, C.; Glomb, M. A. Oxygen-Dependent Fragmentation Reactions during the Degradation of 1-Deoxy-d-Erythro-Hexo-2,3-Diulose. *J. Agric. Food Chem.* **2010**, *58* (9), 5685–5691. https://doi.org/10.1021/jf100140h.

(47) Glomb, M. A.; Henning, C. Formation of Reactive Fragmentation Products during the Maillard Degradation of Reducing Sugars − A Review. In *ACS Symposium Series*; Granvogl, M., Peterson, D., Schieberle, P., Eds.; American Chemical Society: Washington, DC, 2016; Vol. 1237, pp 117–131. https://doi.org/10.1021/bk-2016-1237.ch009.

(48) Thornalley, P. J.; Langborg, A.; Minhas, H. S. Formation of Glyoxal, Methylglyoxal and 3-Deoxyglucosone in the Glycation of Proteins by Glucose. *Biochem J* **1999**, *344 Pt 1* (Pt 1), 109–116.

(49) Jiang, L.; Althoff, E. A.; Clemente, F. R.; Doyle, L.; Röthlisberger, D.; Zanghellini, A.; Gallaher, J. L.; Betker, J. L.; Tanaka, F.; Barbas, C. F.; Hilvert, D.; Houk, K. N.; Stoddard, B. L.; Baker, D. De Novo Computational Design of Retro-Aldol Enzymes. *Science* **2008**, *319* (5868), 1387–1391. https://doi.org/10.1126/science.1152692.

(50) Romero-Rivera, A.; Garcia-Borràs, M.; Osuna, S. Role of Conformational Dynamics in the Evolution of Retro-Aldolase Activity. *ACS Catal.* **2017**, *7* (12), 8524–8532. https://doi.org/10.1021/acscatal.7b02954.

(51) De Raffele, D.; Martí, S.; Moliner, V. Understanding the Directed Evolution of De Novo Retro-Aldolases from QM/MM Studies. *ACS Catal.* **2020**, *10* (14), 7871–7883. https://doi.org/10.1021/acscatal.0c01165.

(52) Ducker, G. S.; Rabinowitz, J. D. One-Carbon Metabolism in Health and Disease. *Cell Metabolism* **2017**, *25* (1), 27–42. https://doi.org/10.1016/j.cmet.2016.08.009.

(53) Pietzke, M.; Meiser, J.; Vazquez, A. Formate Metabolism in Health and Disease. *Molecular Metabolism* **2020**, *33*, 23–37. https://doi.org/10.1016/j.molmet.2019.05.012.

(54) Crossley, S. W. M.; Tenney, L.; Pham, V. N.; Xie, X.; Zhao, M. W.; Chang, C. J. A Transfer Hydrogenation Approach to Activity-Based Sensing of Formate in Living Cells. *J. Am. Chem. Soc.* **2024**, *146* (13), 8865–8876. https://doi.org/10.1021/jacs.3c09735.

(55) Koizumi, K.; Nakayama, M.; Zhu, W.-J.; Ito, S. Characteristic Effects of Methylglyoxal and Its Degraded Product Formate on Viability of Human Histiocytes: A Possible Detoxification Pathway of Methylglyoxal. *Biochemical and Biophysical Research Communications* **2011**, *407* (2), 426–431. https://doi.org/10.1016/j.bbrc.2011.03.041.

(56) Kitamura, Y.; Kawase, M.; Ohmori, S. Formate Excretion in Urine of Rats Fed Dimethylaminoazobenzene-Rich Diets: The Possibility of Formate Formation from D-Lactate. Okayama University Medical School June 2008. https://doi.org/10.18926/AMO/30975.

(57) Nukaya, H.; Inaoka, Y.; Ishida, H.; Tsuji, K.; Suwa, Y.; Wakabayashi, K.; Kosuge, T. Modification of the Amino Group of Guanosine by Methylglyoxal and Other .ALPHA.-Ketoaldehydes in the Presence of Hydrogen Peroxide. *Chem. Pharm. Bull.* **1993**, *41* (4), 649–653. https://doi.org/10.1248/cpb.41.649.

(58) Nakayama, M.; Saito, K.; Sato, E.; Nakayama, K.; Terawaki, H.; Ito, S.; Kohno, M. Radical Generation by the Non-Enzymatic Reaction of Methylglyoxal and Hydrogen Peroxide. *Redox Report* **2007**, *12* (3), 125–133. https://doi.org/10.1179/135100007X200182.

(59) Argilés, J. M. The Oxidation of Methylglyoxal by Mammalian Pyruvate Dehydrogenase. *Archives of Biochemistry and Biophysics* **1989**, *273* (1), 238–244. https://doi.org/10.1016/0003-9861(89)90184-7.

(60) Watkins, N. G.; Neglia-Fisher, C. I.; Dyer, D. G.; Thorpe, S. R.; Baynes, J. W. Effect of Phosphate on the Kinetics and Specificity of Glycation of Protein. *Journal of Biological Chemistry* **1987**, *262* (15), 7207–7212. https://doi.org/10.1016/S0021-9258(18)48224-5.

(61) Li, X.-H.; Xie, J.-Z.; Jiang, X.; Lv, B.-L.; Cheng, X.-S.; Du, L.-L.; Zhang, J.-Y.; Wang, J.-Z.; Zhou, X.-W. Methylglyoxal Induces Tau Hyperphosphorylation via Promoting AGEs Formation. *Neuromol Med* **2012**, *14* (4), 338–348. https://doi.org/10.1007/s12017-012-8191-0.

(62) Patil, G.; Kulsange, S.; Kazi, R.; Chirmade, T.; Kale, V.; Mote, C.; Aswar, M.; Koratkar, S.; Agawane, S.; Kulkarni, M. Behavioral and Proteomic Studies Reveal Methylglyoxal Activate Pathways Associated with Alzheimer's Disease. *ACS Pharmacol. Transl. Sci.* **2023**, *6* (1), 65–75. https://doi.org/10.1021/acsptsci.2c00143.

(63) Miyata, S.; Miyazaki, H.; Liu, B.-F.; Fukunaga, M.; Hamada, Y.; Ueyama, S.; Muramoto, O.; Jiang, Q. Y.; Kusunoki, H.; Uriuhara, A.; Hirota, Y.; Kasuga, M. Activation of MAP Kinase Superfamily

Signaling Pathways by Methylglyoxal. *International Congress Series* **2002**, *1245*, 87–89. https://doi.org/10.1016/S0531-5131(02)00913-5.

(64) Dafre, A. L.; Schmitz, A. E.; Maher, P. Methylglyoxal-Induced AMPK Activation Leads to Autophagic Degradation of Thioredoxin 1 and Glyoxalase 2 in HT22 Nerve Cells. *Free Radical Biology and Medicine* **2017**, *108*, 270–279. https://doi.org/10.1016/j.freeradbiomed.2017.03.028.

FIGURES

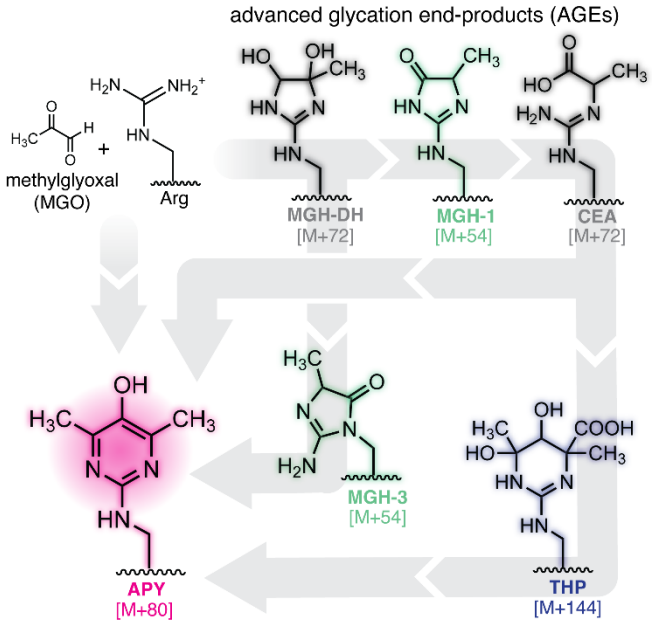

Figure 1. Overview of MGO-derived advanced glycation end-products. In addition to APY, these include the methylglyoxal-derived hydroimidazolone isomers (MGH-1, -2, & -3), dihydroxyimidazolidine (MGH-DH), carboxyethylarginine (CEA), and tetrahydropyrimidine (THP). Several possible pathways for APY formation have been proposed (gray arrows).

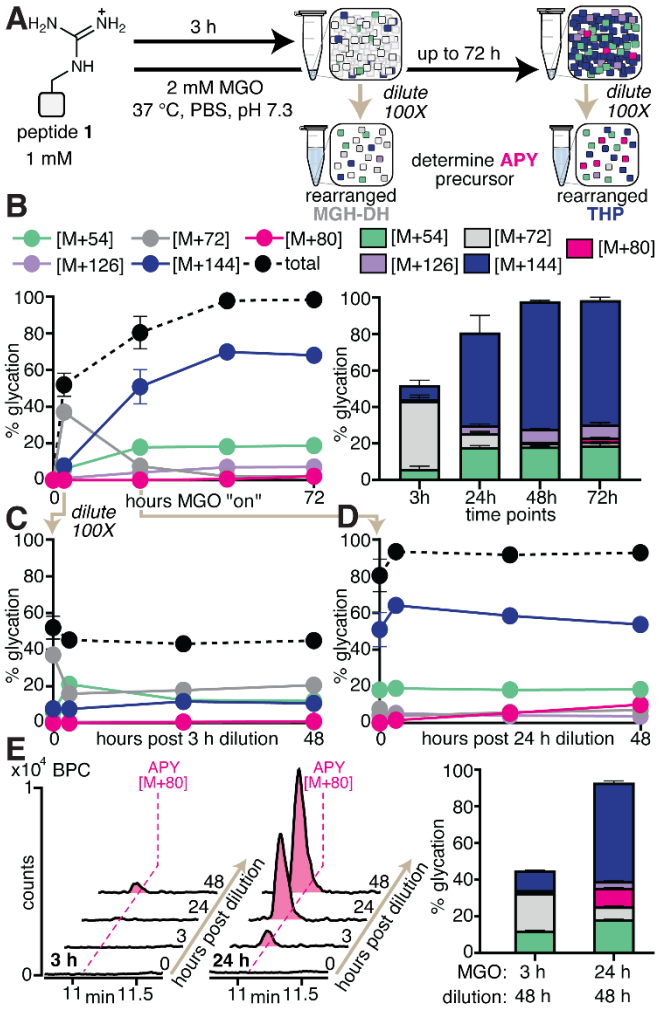

Figure 2. THP is a Precursor to APY. (A) General scheme showing the experimental setup used to determine the APY precursor. **(B)** Peptide **1** (1 mM) was treated with 2 mM MGO and incubated for up to 72 h (labeled as "hours MGO "on"), as shown in a time course (left) and stacked bar graph (right) showing AGE distributions. **(C)** After 3 h, (when MGH-DH became the predominant adduct) or **(D)** after 24 h (when THP became the predominant adduct), the reaction was diluted 100X in the same buffer and incubated for additional 48 h post dilution ("hours post dilution"). Since dilution markedly slows MGO addition, this protocol diminishes new AGE formation on already glycated peptides, enabling the clear observation of rearrangements between AGEs. **(E)** Representative base peak chromatograms (BPC) (left) and bar graph (right) for peptide **1** at several post dilution time points (n≥3 for all reactions). A significant increase in APY [M+80] (magenta) levels was observed at 48 h post dilution of the 24 h time point when compared to that of the 3 h timepoint. These results suggest that THP [M+144] (blue), and not MGH-DH (gray), is a precursor for APY.

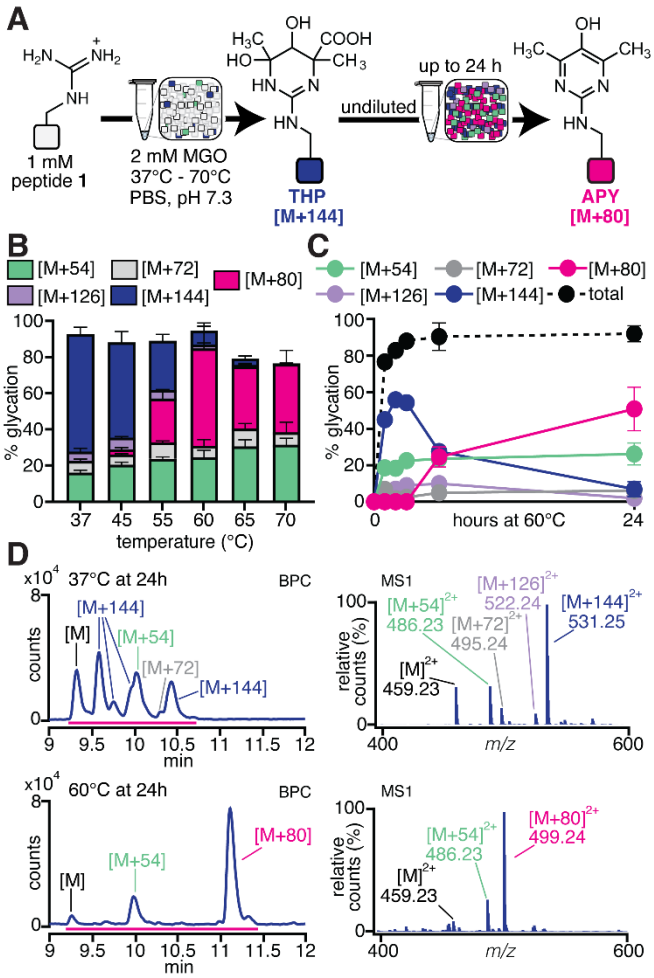

Figure 3. APY is a stable AGE. (A) Seeking to increase APY levels, we conducted a temperature scan by treating peptide **1** with 2 mM MGO over a range of temperatures from 37 °C to 60 °C. The reaction was incubated for 24 h undiluted, and AGE distributions were assessed *via* liquid chromatography-mass spectrometry (LC-MS) analysis. **(B)** Stacked bar graph showing AGE distributions for peptide **1** treated with MGO for 24 h at 37 °C, 45 °C, 55 °C, 60 °C, 65 °C, and 70 °C. At 55 °C, we began to observe a notable increase in APY [M+80] (magenta) that was concomitant with reduced THP [M+144] (blue) levels. APY was the predominant adduct in just 24 h at 60 °C. **(C)** Time course of peptide **1** glycation reactions at 60 °C, extended over several time points (1 h, 2 h, 3 h, 6 h, and 24 h) (n≥3 for all reactions). Under these conditions, THP quickly became the predominant adduct in just 2 h, then decreased precipitously between 2 h and 24 h. During this same time frame, a dramatic increase in APY levels was observed, confirming THP as a precursor to APY. **(D)** Representative BPCs and MS1 spectra for the glycation reaction of peptide **1** after 24 h incubation at 37 °C (top) and 60 °C (bottom). Together, these results provide conditions at which APY becomes the predominant AGE, suggesting that APY formation likely involves a relatively high energy activation barrier that can be overcome by the addition of heat.

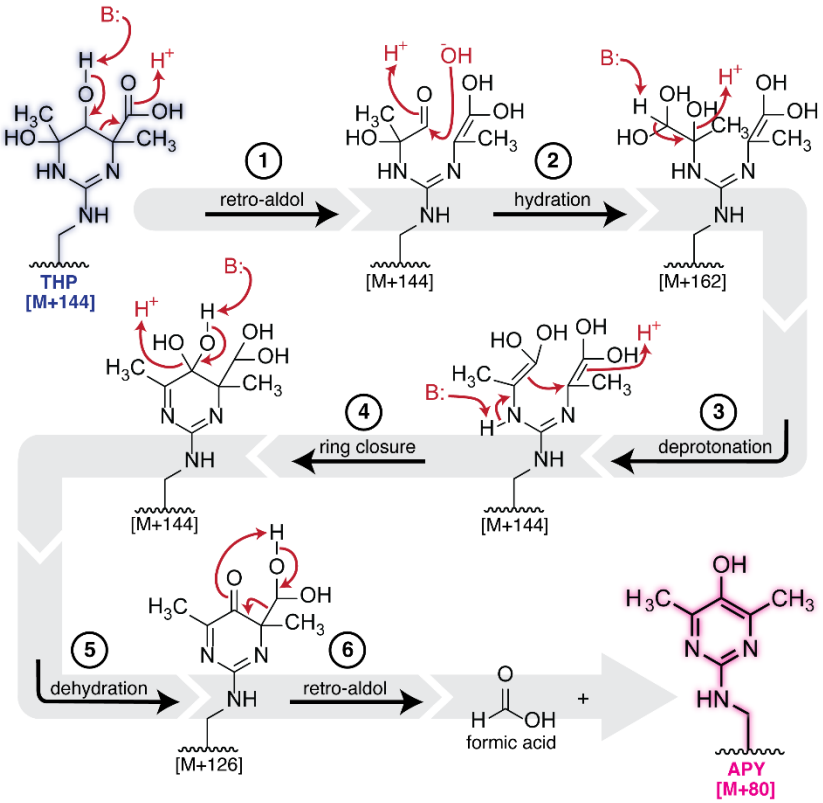

Figure 4. Proposed Mechanism for APY Formation. We propose that THP can rearrange into APY via a retro-aldol step (1), followed by hydration (2), then deprotonation (3) and ring closure (4), another dehydration step (5), and finally a retro-aldol step (6) that also releases formic acid. as a byproduct.

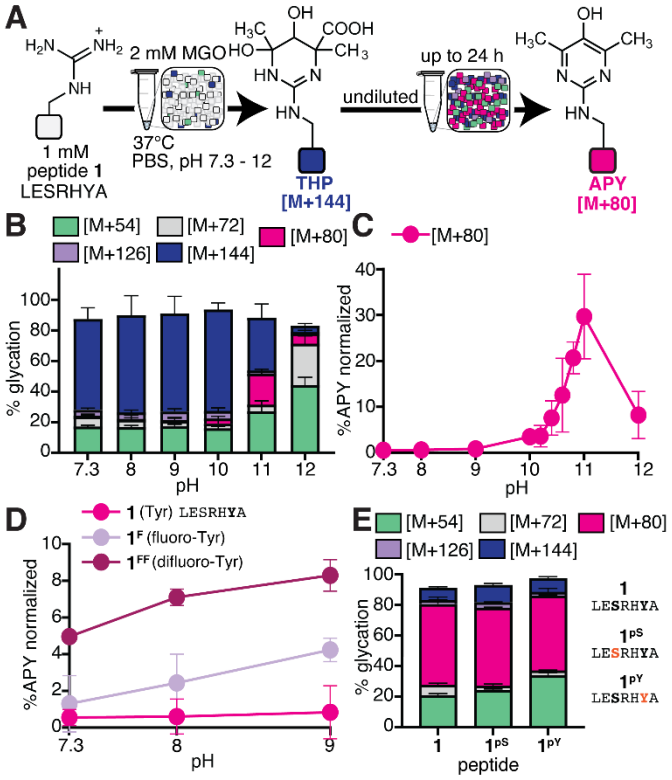

Figure 5. A Nearby General Base Facilitates the Rearrangement of THP into APY. (A) General scheme depicting a pH scan used to evaluate the features that promote APY formation. Peptide **1** (1 mM) was treated with 2 mM MGO using pH-adjusted phosphate buffered saline (PBS) in a pH range of 7.3—12. The reaction was incubated for 24 h undiluted at 37 °C. **(B)** Stacked bar graphs showing AGE distributions, as assessed by liquid chromatography-mass spectrometry (LC-MS) analysis. **(C)** Between pH 10 and 11, we observed a marked jump in APY [M+80] (magenta) levels, as shown by proportional APY levels that were normalized to the total amount of glycation observed for MGO-treated peptide **1** across a narrower pH range between pH 10 and 11 at 0.2 increments. **(D)** To further test the hypothesis that Tyr phenoxide plays an active role in APY formation, we conducted glycation reactions on variants of peptide **1**, including peptide $\mathbf{1^{F}}$ (fluoro-Tyr in lieu of Tyr) and peptide $\mathbf{1^{FF}}$ (difluoro-Tyr in lieu of Tyr). Here, proportional APY levels were normalized to the total amount of glycation to account for differences in total glycation. At pH 7.3 and 37 °C, % APY was the greatest for peptide $\mathbf{1^{FF}}$ (pK_a 7.2), followed by peptide $\mathbf{1^{F}}$ (pK_a 8.4), and then peptide **1** (pK_a 10.3), consistent with our hypothesis. **(E)** Stacked bar graphs showing AGE distributions for glycation reactions with peptide **1**, peptide $\mathbf{1^{pS}}$ (pSer in place of Ser, pK_{a2} 5.6), and peptide $\mathbf{1^{pY}}$ (pTyr in place of Tyr, pK_{a2} 5.9) at pH 7.3 and 60 °C (24 h incubation) (n≥3 for all reactions). Despite the introduction of up to two negative charges which has been reported to hamper glycation, absolute APY levels and total glycation levels remained virtually identical for these phosphorylated variants. Together, these results demonstrate the importance of a nearby general base to facilitate APY formation and suggest that nearby phosphorylated residues can also aid glycation.

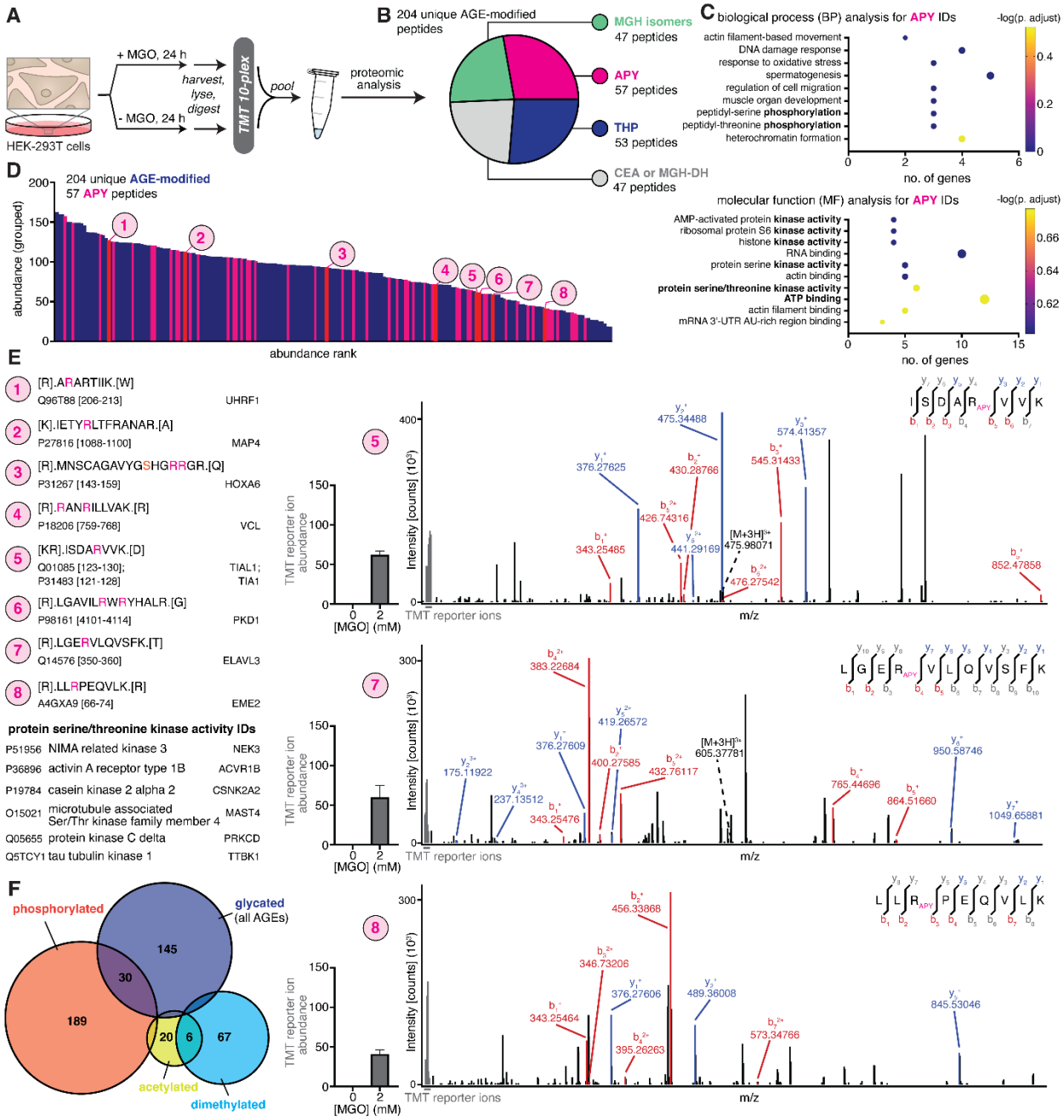

Figure 6. Proteomic Analysis on MGO-treated Cells Reveal a Connection between APY and Cellular Phosphorylation Events. Given that our proposed mechanism for APY formation was supported by *in vitro* peptide data, we set out to investigate APY formation in a cellular context, along with other common MGO-modified AGEs. **(A)** General scheme describing our proteomic workflow on HEK-293T cells treated with or without 2 mM MGO for 24 h. Whole cell lysates were trypsin-digested, labeled with TMT isobaric tags, and analyzed in a quantitative bottom-up workflow. The untreated sample was used as a frame of reference to identify any AGE increase in the treated condition. **(B)** Pie chart showing a set of 204 unique peptides with AGE-modified Arg in the MGO-treated condition, consisting of 57 APY-, 53 THP-, 47 MGH-, and 47 CEA/MGH-

DH-containing peptides. **(C)** DAVID Gene Ontology (GO) analysis was performed for protein IDs associated with the APY set using a 0.05 false discovery rate (FDR). Both the biological process (BP) and molecular function (MF) analyses revealed phosphorylation-related terms (bolded text) that are unique to the APY set. **(D)&(E)** The abundance (grouped) for APY-containing peptides (magenta) was ranked and displayed atop the abundance of other AGE-containing peptides (blue). Eight statistically significant increased APY-containing peptides (red) are numbered 1-8. Protein IDs from the protein serine/threonine kinase activity term are also shown in **(E)**. Representative b/y ion spectra and TMT reporter ion abundance quantitation for three of the high confidence APY hits are shown. **(F)** Venn diagram showing overlapping IDs between AGEs or other common Arg modifications (dimethylation and acetylation) and phosphorylation. Compared to dimethylated and acetylated IDs, glycated IDs exhibited a substantial overlap (30 IDs) with phosphorylated IDs, suggesting a connection between AGE formation and cellular phosphorylation events.